Annals of Anatomy 234 (2021) 151624

Contents lists available at ScienceDirect

Annals of Anatomy

journal homepage: www.elsevier.com/locate/aanat

RESEARCH ARTICLE

The anatomical reliability of the superficial circumflex iliac artery perforator (SCIP) flap

Cédric Zubler[a,b], David Haberthür[a], Ruslan Hlushchuk[a], Valentin Djonov[a], Mihai A. Constantinescu[b], Radu Olariu[b,*]

[a] Institute of Anatomy, University of Bern, Baltzerstrasse 2, 3012 Bern, Switzerland
[b] Department of Plastic and Hand Surgery, Inselspital University Hospital Bern, Freiburgstrasse, 3010 Bern, Switzerland

ARTICLE INFO

Article history:
Received 16 May 2020
Received in revised form 23 August 2020
Accepted 12 October 2020

Keywords:
Superficial circumflex iliac artery
Deep branch
Superficial branch
Perforator flap
Superficial circumflex iliac artery perforator flap
Reconstructive surgery

ABSTRACT

Introduction: In order to achieve a satisfactory functional and aesthetic result a thin skin flap is often required in surgical reconstruction of various body regions. Perforator flaps based on either the superficial or deep branch of the superficial circumflex iliac artery (SCIA) have been used for this purpose mainly in the Asian population. Recently the superficial plane has been established as a new way of elevating the flap. Anatomical studies and details of this new flap are lacking.
Material and methods: Wide areas were harvested subfascially from the groin of Thiel-fixated cadavers. Both deep and superficial branches of the superficial circumflex iliac artery were carefully dissected and individually injected with μAngiofil. After CT-imaging the flaps were raised on the superficial plane, perforators were marked and the flaps subsequently rescanned. High-resolution images of regions of interest were taken using micro-CT.
Results: A total of 21 flaps were harvested and analyzed. Both the deep and superficial branch provided more than three perforators per branch, however, the deep branch based flap was significantly larger (202 vs. 112 cm^2, $p < 0.01$) and had a longer pedicle (9.1 vs. 6.6 cm, $p < 0.01$). Raising the flap in the superficial plane reliably reduces bulk and increases homogeneity.
Conclusions: The SCIP flap appears to have a reliable vascular blood supply. The SCIA and its main branches and perforators have a consistent vascular pattern. The deep branch of the SCIA has the anatomic potential to be the preferred pedicle in case larger flaps with longer pedicles are necessary.

1. Introduction

Since the first description of the groin flap based on the superficial circumflex iliac artery (SCIA) by McGregor and Jackson in 1972 and its subsequent application as the first successful free flap (Daniel and Taylor, 1973) the groin region was hailed as an almost disposable minimal-morbidity donor site due to the easy concealment of the donor scar and minimal morbidity of flap harvesting (Hough et al., 2004). However, the short and small caliber of the vascular pedicle, the bulkiness of the flap and the variability of the vascular anatomy (Hsu et al., 2007) lead to decreasing popularity of the groin flap as new flaps were described.

The recent advances in dissection and clinical use of perforator based flaps revived interest in the inguinal donor site with the landmark works of Koshima et al. (2004) and Hong et al. (2014) describing the superficial iliac artery perforator (SCIP) flap and showing the possibility of raising a thin flap with a longer, more reliable pedicle.

Recently multiple reports including large case series showed the successful use of the SCIP flap for the reconstruction of a variety of body regions, including head and neck (Feng et al., 2017; Goh et al., 2015; He et al., 2016; Hsu et al., 2007), upper extremity (Feng et al., 2017; Goh et al., 2015; Hsu et al., 2007; Kim et al., 2015), trunk region (Feng et al., 2017; Goh et al., 2015), lower limb (Feng et al., 2017; Goh et al., 2015; Hong et al., 2014, 2013; Hsu et al., 2007; Kim et al., 2015; Koshima et al., 2004; Myung et al., 2017), genitalia (penis, scrotum) (Han et al., 2016; Koshima et al., 2006) and even the external auditory canal (Iida et al., 2013). Most of these studies were performed in the Asian population.

Despite increasing clinical use, thorough anatomical studies on the specific implications of the new techniques in planning and usage of SCIP-flaps are still lacking, especially in the Western population. A recent anatomical study performed in a European anatomical institute has provided some more insight into the vas-

* Corresponding author.
E-mail address: radu.olariu@insel.ch (R. Olariu).

https://doi.org/10.1016/j.aanat.2020.151624

cular anatomy of the SCIP flap with special focus on the possibility of chimeric flaps including muscle and bone, however, the skin flap has been still based on superficial branch perforators (Yoshimatsu et al., 2019a, 2019b). Despite some increase in anatomical knowledge, variations and uncertainties in vascular blood supply remain challenging and the SCIP-flap has not yet gained broad acceptance at least outside Asia. The aim of this study is to thoroughly investigate the anatomical knowledge and understanding regarding the cutaneous SCIP flap and thereby promote the safe application and acceptance of this promising flap.

2. Material and methods

2.1. Anatomical dissection

A total of 21 flaps were harvested as wide areas of tissue from the groin of Thiel-fixated (Bangerter et al., 2017; Thiel, 1992) cadavers as illustrated in Fig. 1. The use of the human cadaveric material was conducted according to the guidelines of the Swiss Academy of Medical Sciences. Donors formally agreed to the use of body parts for research purposes by signing the donation forms.

The age, gender, BMI and skinfold thickness measured 2.5 cm above the iliac crest were recorded for each specimen. The anterior superior iliac spine (ASIS) and pubic tubercle were marked as points of orientation and the flaps subsequently harvested beneath the deep fascia in order to ensure the inclusion of all relevant vessel branches including a long segment of the femoral artery with the emergence of the superficial circumflex iliac artery (SCIA). The superficial circumflex iliac artery was carefully dissected at its origin until the division into deep and superficial branch was identifiable. After test-perfusion with phosphate-buffered saline (PBS) the branches were cannulated and individually injected with μAngiofil (Fumedica AG, Muri, Switzerland) (Hlushchuk et al., 2018; Schaad et al., 2017). After an overview CT-Scan (see method below) the flaps were raised at the level of the superficial fascia. Taking advantage of the colored and hardened contrast-agent, all superficial plane perforators were marked with metal rings during this surgical step and a second CT-Scan was performed. Additional high-resolution images (micro-CT) of regions of interest were taken in both planes (see method below).

2.2. Imaging studies

2.2.1. CT-Scan

An overview CT-Scan was performed on a Siemens Somatom Definition AS 64 (Siemens Healthcare GmbH, Erlangen, Germany). The x-ray source was set to 140 kVp, the resulting images had an isotropic voxel size of 0.6 mm, with their gray scale values scaled to Hounsfield units with a window center of 300 and a window width of 100. After the first CT scan, the flaps were raised on the superficial plane (at the level of the superficial fascia) and a second CT-scan was performed.

2.2.2. Micro-CT scan

High-resolution micro-CT images of regions of interest were recorded with either a SkyScan 2211: Multiscale X-ray Nano-CT System or Bruker SkyScan1272 high resolution microtomography system (both from Bruker microCT, Kontich, Belgium).

On the SkyScan 2211 system, the the X-ray source was set to high power mode with a voltage of 60 kV and a current of 144 μA. We recorded a set of 1086 projections of 3776 × 1536 pixels (two offset projections with 1920 × 1536 pixels merged to one) at every 0.2° over a 180° sample rotation; every projection was exposed for 100 milliseconds, three projections were averaged to reduce noise. Three scans were recorded along the rotation axis to cover the whole sample. This resulted in a scan time of about one hour and 45 min and an isometric voxel size of 56 μm in the final data set.

On the SkyScan 1272 system, the the X-ray source was set to a voltage of 100 kV and a current of 100 μA. We used a 0.11 mm thick Copper filter to shape the spectrum of the X-ray source. A set of 337 projections of 3432 × 818 pixels (three offset projections with 1224 × 818 pixels merged to one) was recorded at every 0.6° over a 180° sample rotation; every projection was exposed for 2.9 s, five projections were averaged to reduce noise. Six scans were recorded along the rotation axis to cover the whole sample. This resulted in a scan time of about four hours and 25 min and an isometric voxel size of 21.1 μm in the final data set.

On both systems the projection images were reconstructed into a 3D stack of images with NRecon (Bruker, Version: 1.7.0.4).

2.3. Image analysis

The acquired Datasets were then reconstructed and analyzed using ImageJ2 (Rueden et al., 2017) (version: 2.0.0-rc-67/1.52d, Build: 1762a07c5c.) and Imaris (version 9.0.2, Build 44695 for ×64, Bitplaine AG, Zurich, Switzerland). With the aid of these image analysis tools a multi-step process was implemented to ensure comparability between the different flaps. On the mathematical basis of affine transformation all flaps were rotated and scaled to a set standard length and incline of the inguinal ligament using the ASIS and pubic tubercle as anchor points. When absolute values concerning length or square measures were needed, all measurements were taken on the original images to avoid any distortion of the results.

Based on these reconstructions and scans the following parameters were measured:

- number of superficial plane perforators per branch and their relative position to the ASIS and pubic tubercle
- maximal pedicle length (measured from the main superficial plane perforator to the origin of the vessel from the femoral artery)
- area of the perfused primary vascular tree per respective branch. The areas of those angiosomes were then transformed onto the settings of the standard flap as described above and stacked in order to determine the area of maximal overlay (100% perfused area)
- layer thickness of the superficial as well as the deep plane. This was performed in the area that was perfused in all flaps (100% perfused area) and the total area of the individual branch's angiosome.
- average local thickness of the different planes. This parameter was calculated by summing up the thickness values of the standardized flaps for every pixel and dividing the total by the number of flaps overlapping in this location.

After excluding potential variance heterogeneity with an F-test, statistical comparisons were made using two-tailed student's *t*-tests. If the layer thickness was measured on both planes in the same flap and location, paired two-tailed student's *t*-tests were used.

All numbers are expressed as means ± standard deviation with the exception of age, BMI and skinfold thickness where the means and ranges are described.

3. Results

The 21 flaps included eight female and 13 male specimens. The mean age of the cadavers was 83.8 years (range 71–93 years), mean BMI 22.7 kg/m^2 (range 20.5–24.9 kg/m^2) and the mean skinfold

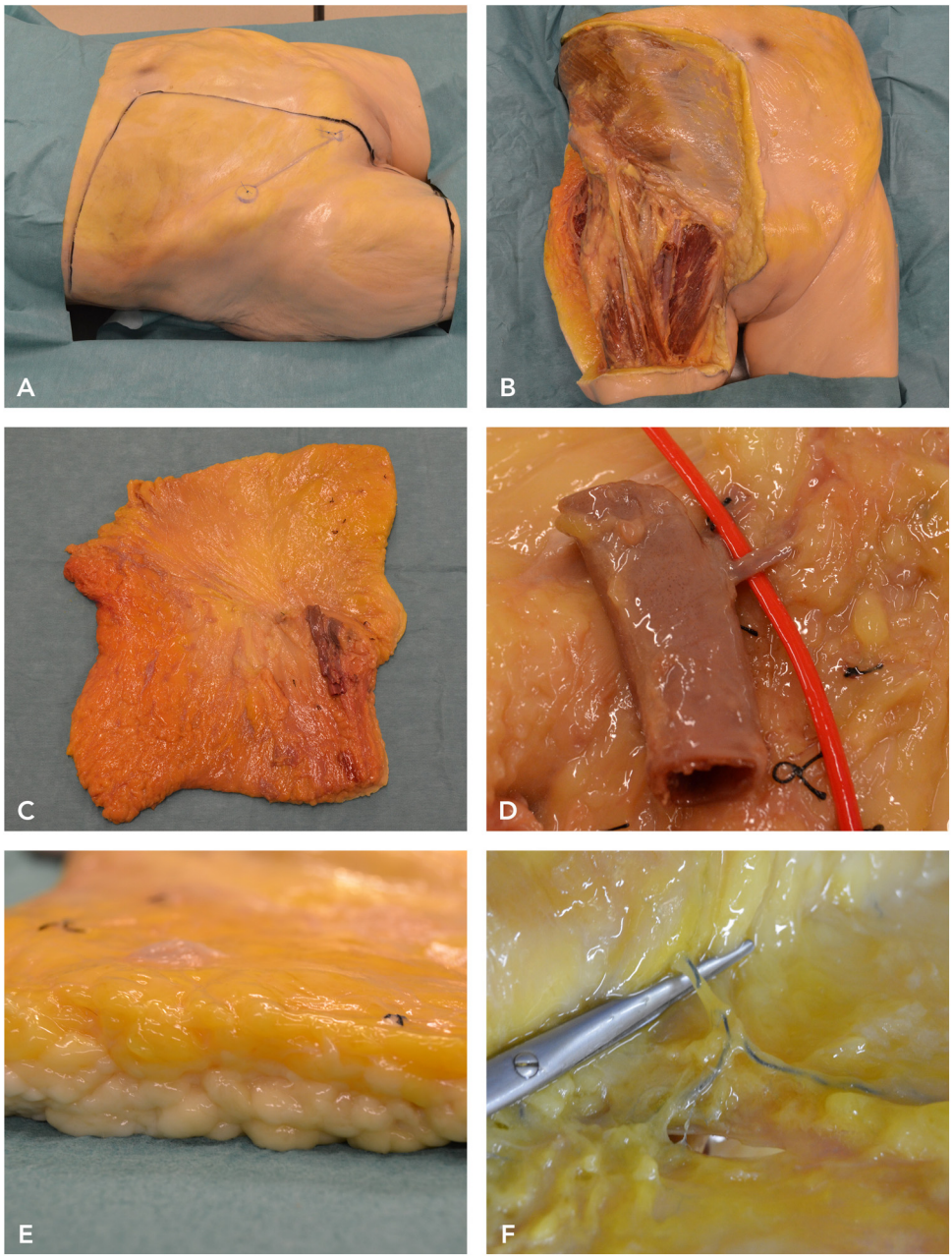

Fig. 1. A. Surface marking of the anatomical specimen as well as the ASIS and pubic tubercle as points of reference. B. Aspect of the deep surface of the abdomen and thigh after specimen raising showing subfascial dissection. C. Aspect of the deep side of the dissected specimen with a long segment of the femoral artery. D. Example of the dissection of the SCIA branches with the deep (above the vessel loop) and superficial (cranially under the vessel loop) SCIA branch. E. Superficial and deep fat are clearly distinguishable after elevation of the flap. F. Example of a perforator detected during superficial plane dissection. The μAngiofil-filled and hardened small perforators are easily detected.

thickness (measured 2.5 cm above the iliac crest) was 11 mm (range 6–16 mm).

3.1. General and descriptive vascular anatomy

The SCIA originated from the common femoral artery or the superficial femoral artery in all specimen. Both the superficial and the deep branch of the SCIA could be identified in each cadaver. The deep branch was always found to lie subfascially and never to course through the sartorius muscle. Only in one instance a sizeable transmuscular skin perforator through the sartorius muscle originating from the deep branch was encountered. Despite its caliber, this perforator did not represent the main perforator of the branch.

3.1.1. Superficial branch

The superficial branch penetrates the deep fascia almost directly after its origin from the SCIA and then runs in the deep fat in a latero-cranial direction. It usually crosses the inguinal ligament in its lateral third (Fig. 3). After giving off a number of perforators the branch itself penetrates the superficial fascia, becoming the main perforator, which continues its course in the superficial fat in a more or less straight line (Fig. 2). Both in the deep and superficial plane this branch gives off vessels to both sides.

3.1.2. Deep branch

The deep branch runs subfascially over a longer distance and regularly gives off nurturing vessels to deep inguinal lymph nodes, deep fascia and also the sartorius muscle (Fig. 3). At the lateral bor-

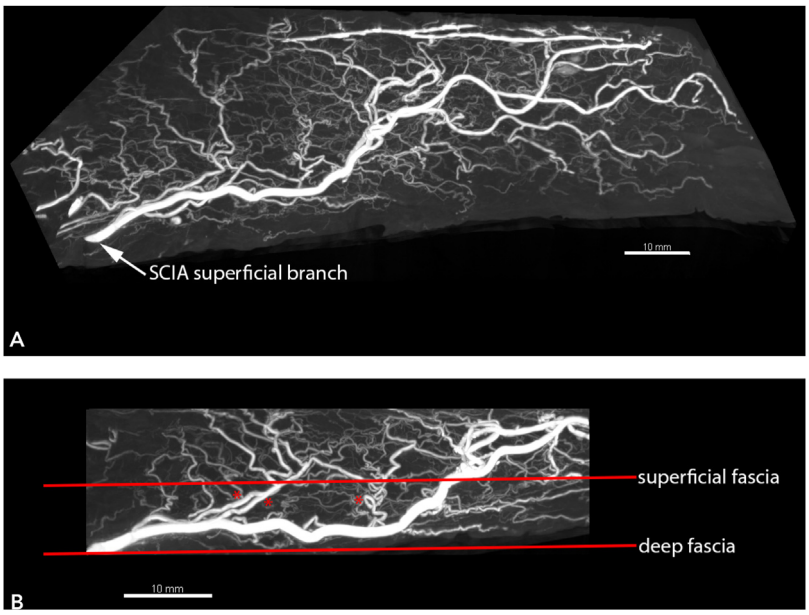

Fig. 2. μCT-overview illustrating the typical course of the superficial branch of the SCIA. A. 3D overview. B. 2D section showing a number of smaller caliber perforators (marked here with red asterisks) branching off the vessel before the branch itself penetrates the superficial fascia, becoming the main perforator. The perforators present a tortuous course which could indicate the vascular adaptability of the flap to increased tension at the time of recipient site inset. The main perforator continues its course in the superficial fat, giving off multiple branches to the overlaying subdermal plexus. (For interpretation of the references to colour in this figure legend, the reader is referred to the web version of this article.)

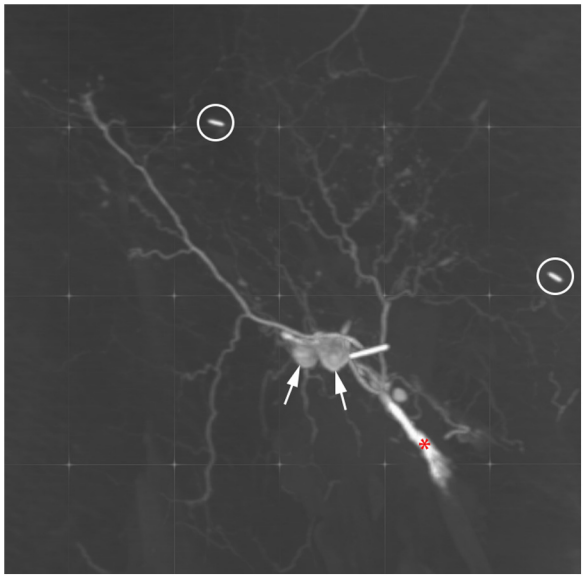

Fig. 3. Conventional CT-scan showing the general patterns of the typical course of both SCIA-branches in relation to one another. The white circles indicate the ASIS (left) and pubic tubercle (right), the red asterisk marks the injection cannula. The superficial branch runs in a latero-cranial direction towards the ASIS, normally crossing the inguinal ligament medially to this fixpoint. The deep branch on the other hand runs infero-laterally and its major branches are often directed in an inferior or slightly lateral direction with only minor vessels sprouting towards the superficial branch. Furthermore, the deep branch regularly gives off supplying veFissels in its medial portion to lymph nodes (indicated by the white arrows) located in the deep fat. (For interpretation of the references to colour in this figure legend, the reader is referred to the web version of this article.)

der of this muscle the main vessel normally penetrates both fasciae in quick succession due to the lack of deep fat in this region. Its major side branches predominantly run in an inferior and lateral direction. This is further also illustrated by the distribution of its perforators (Fig. 4).

3.2. Angiosomes and perforators

The mean total area of the perfused angiosome was significantly larger for the deep branch (202 ± 53.8 cm^2) compared to the superficial branch (112 ± 46.3 cm^2) (p-value < 0.01). This was also reflected in significantly longer (14.6 ± 2.5 cm superficial branch vs. 19.7 ± 3.6 cm deep branch, p-value < 0.05) and wider (9.7 ± 2.7 cm superficial branch vs. 13.7 ± 3.3 cm deep branch, p-value < 0.05) flaps on average for the deep branch. There was no significant difference in the 100% perfusion-area (Fig. 4) which was much smaller than the average total angiosome (mean area of the 100%-perfusion-area: 34.0 ± 8.8 cm^2 superficial branch vs. 34.8 ± 6.0 cm^2 deep branch, p-value = 0.68). The total angiosome of the superficial branch extends further along the axis of its main vessel in craniolateral direction while the deep branch angiosome extends predominantly in an inferio-lateral direction along its major side branches.

There was no significant difference between the number of superficial plane perforators per branch. (3.4 ± 0.9 perforators of the superficial branch vs. 3.6 ± 1.1 perforators of the deep branch, p-value = 0.61). However, the perforators of the deep branch were on average significantly more distant from each other (distance from the centroid: 2.8 ± 0.8 cm superficial branch, 3.9 ± 1.0 cm deep branch, p-value < 0.01), correlating with the larger angiosome they supply.

The location of the superficial plane perforators from both branches are mapped in Fig. 4 with the main perforator of every branch highlighted showing a clear medio-lateral division. The superficial branch's main perforators gather around the lateral half of the inguinal ligament while the main perforators from the deep branch can be found in a region latero-inferior to the ASIS and lateral to the lateral border of the sartorius muscle.

The maximal pedicle length measured from the main superficial plane perforator to the origin of the vessel from the femoral artery was significantly longer for the deep branch than the superficial branch (mean pedicle length: 6.6 ± 1.1 cm superficial branch, 9.1 ± 1.0 cm deep branch, p-value < 0.01).

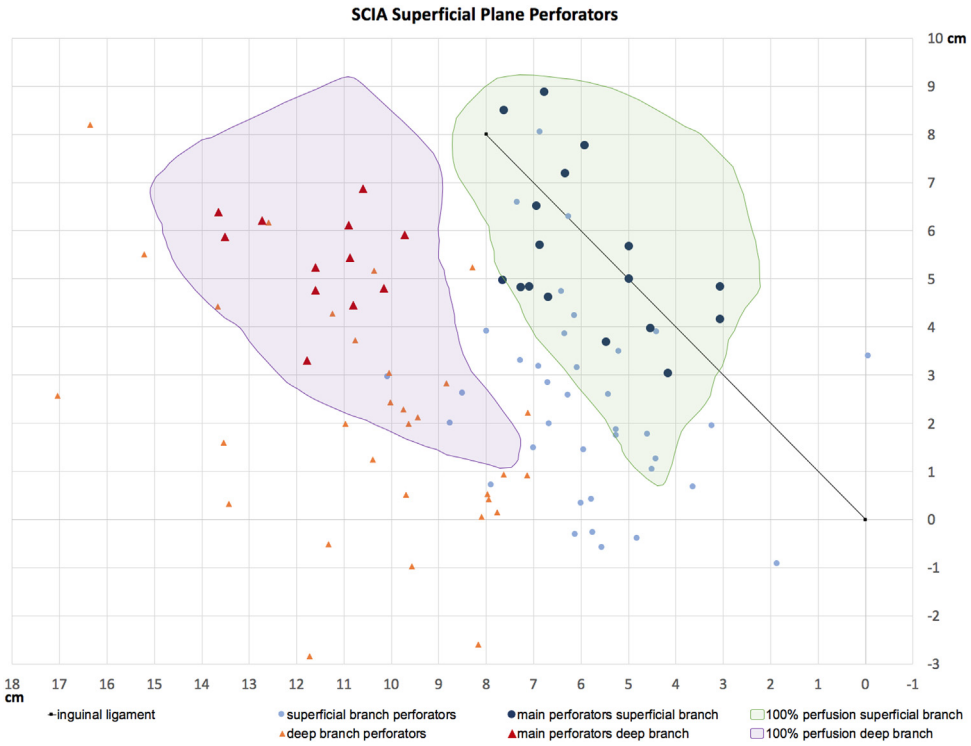

Fig. 4. Mapping of the location of the superficial plane perforators from both the superficial and deep branches of the SCIA. The division into medial and lateral perforators is clearly noticeable. While the main perforators of the superficial branch aggregate around the lateral part of the inguinal ligament, the deep branch main perforators cluster in a region latero-inferior to the ASIS. Furthermore, the highlighted regions illustrate the area that were always perfused by the respective branch.

3.3. Layer thickness

The flap thickness of the whole specimen is significantly reduced when the superficial plane elevation is used (mean thickness of whole specimen: 12.2 ± 2.4 mm deep plane vs. 7.3 ± 1.3 mm superficial plane, p-value < 0.001. Mean reduction overall: 4.9 ± 1.4 mm). The comparative analysis of the layer thickness between the two SCIA branches was performed on the one hand for the 100% perfusion-area and on the other hand for the total branch angiosomes:

3.3.1. 100% perfusion-area

Within this area, the deep branch offers a significantly thinner flap on the deep plane (mean thickness: 9.7 ± 2.7 mm superficial branch, 8.6 ± 1.4 mm deep branch, p-value < 0.01) and on the superficial plane (mean thickness: 6.1 ± 1.4 mm superficial branch, 5.6 ± SD 1.3 mm deep branch, p-value < 0.05). The reduction in layer thickness by elevating the flap on the superficial plane is significantly higher for the superficial branch area (average reduction: 3.6 ± 1.9 mm superficial branch, 3.0 ± 1.2 mm deep branch, p-value < 0.05). Most of the reduction in thickness is gained in the medial area of the flap (Fig. 5-C).

3.3.2. Total branch angiosome

Here the superficial branch angiosome is significantly thinner on the deep plane (mean thickness: 9.0 ± 1.8 mm superficial branch, 11.7 ± 0.9 mm deep branch, p-value < 0.05) as well as on the superficial plane (mean thickness: 5.8 ± 0.9 mm superficial branch, 7.5 ± 1.1 mm deep branch, p-value < 0.01) compared to the deep branch angiosome. There is no significant difference in the reduction of thickness between the two branches by elevating the flap on the superficial fascia.

Fig. 5 illustrates the local average thickness of the different layers in the groin and circumjacent regions.

The subfascially harvested flap (Fig. 5-A) shows a steady decrease in thickness along the inguinal ligament from medial to lateral. With its minimum around the ASIS, this plane subsequently offers a thin area of tissue around the contour of the iliac crest and becomes thicker with increasing distance from this anatomical landmark in every direction.

The superficially harvested flap (Fig. 5-B) shows a somewhat similar pattern in the distribution of the fat content but with a markedly enlarged region of thin tissue. The superficial plane is overall significantly less variable in its thickness (mean variance of layer thickness: 4.4 ± 1.8 superficial plane, 19.2 ± 7.3 deep plane, p-value < 0.01).

Fig. 5-C, representing the local amount of deep fat (plus deep fascia tissue), highlights the regions where the difference between the two planes is substantial. While the deep fat is prominent in the upper thigh, in the abdominal and towards the gluteal region, it is practically nonexistent around the ASIS and iliac crest.

4. Discussion

The SCIP-flap has evolved from the groin flap in the search for a super thin cutaneous flap. Its benefits include a donor-site with low morbidity that can be primarily closed and is easily concealed, the skin area is mostly hairless and the flap can be adjusted in its thickness from super thin to bulky, depending on the plane of elevation used (Iida et al., 2014). Furthermore, it can also be harvested as a composite flap if necessary and include lymph nodes, nerve, bone or fascia (Iida, 2014). These advantages have led to the SCIP-flap lately being described as the new workhorse flap for different reconstructive needs (Feng et al., 2017; Goh et al., 2015). Nevertheless, this flap has not yet gained broad acceptance. This is mainly due to the perceived anatomical variations in this region and their unclear impacts on the new techniques.

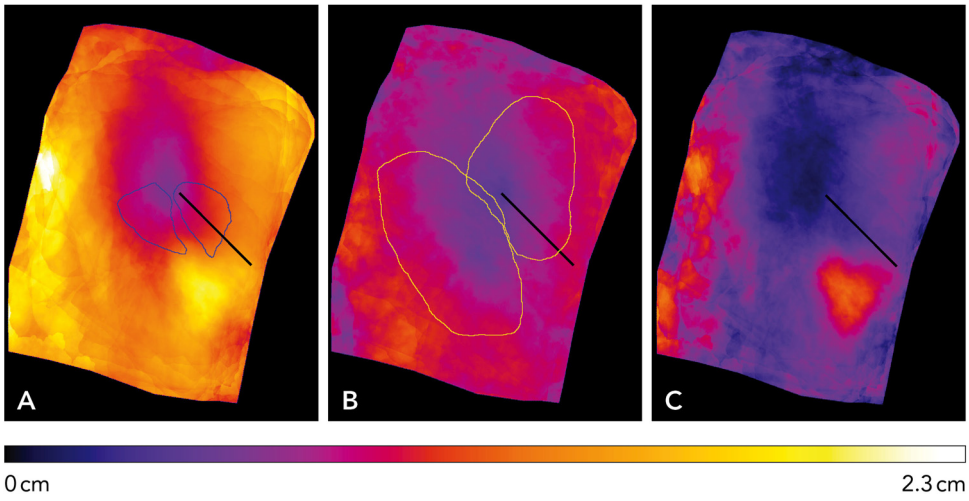

Fig. 5. Maps of the average layer thickness in and around the area in which the SCIP flaps are normally harvested. The black bar represents the inguinal ligament connecting the ASIS (left) and pubic tubercle (right). The 100% perfusion areas of both branches are marked with blue outlines in A. The yellow contours in B illustrate examples of the typical whole branch angiosomes. A. Full thickness flap thickness (raised on the deep plane), B. Flap thickness after superficial plane harvest. C. Subtraction of thickness B from thickness A, therefore illustrating the average local amount of deep fat. (For interpretation of the references to colour in this figure legend, the reader is referred to the web version of this article.)

We have performed a thorough anatomical vascular injection-based study using new state of the art methods in order to try and overcome some of the uncertainties still present in the inguinal region's vascular anatomy. In the past, various vascular injection techniques have been used in the study of perforator flaps to answer similar questions (Bergeron et al., 2006). While offering important insights into the vasculature of different tissues, these techniques are often limited to two-dimensional illustrations of the respective main stem vessels. In addition, some of the most commonly used techniques rely on lead oxide as contrast agent which is highly toxic and potentially harmful if handled incorrectly.

In our study, we applied a new contrast agent in SCIP-flaps harvested from Thiel-fixated cadavers in an effort to enhance the anatomical knowledge about the vasculature and perfusion. The recently introduced microCT-based angiography employing μAngiofil, permit 3D-visualization of the entire vasculature down to the capillary level and in addition rapid estimation of the vessel size distribution (Schaad et al., 2017). μAngiofil is a polyurethane based contrast agent i.e. remains solid but elastic within the vessels, which represent a possibility for alternating dissections and microCT visualizations of the same vessels and the same site of interest. This in combination with the Thiel-embalming methodology, i.e. realistic color, texture conservation and preservation of biomechanical properties (Bangerter et al., 2017) serve as a unique opportunity for advanced microdissection and visualization of the vasculature. While conventional CT-scans enable us to acquire 3D representations of the vascular tree, those images are still restricted to approximately the same resolution reached in older studies (Bergeron et al., 2006). In order to overcome this limitation, we added micro-CT-scans of certain regions of interest, which offer an outstanding level of detail (Fig. 6).

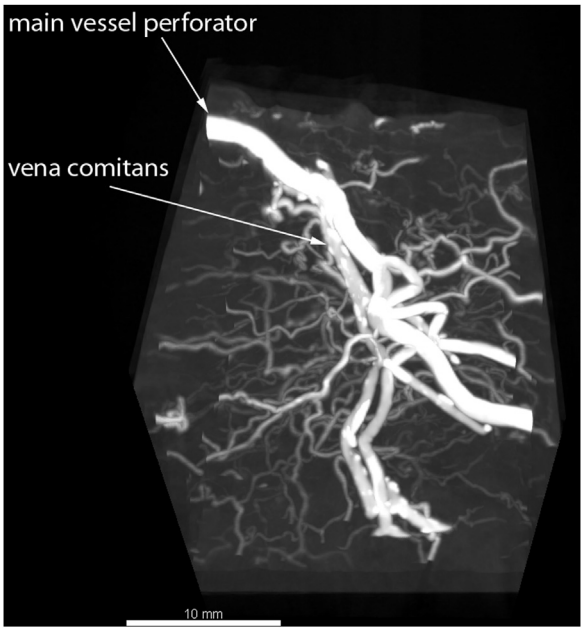

Fig. 6. In combination with μAngiofil the micro-CT-scans allow for very high-resolution imaging and in-depth analysis of regions of interest. Here a superficial plane perforator is illustrated. The arterial vessel is clearly distinguishable from its accompanying vena comitans.

4.1. General and descriptive vascular anatomy

There are multiple conflicting reports on the exact point of emergence of the SCIA from the femoral artery system (Gandolfi et al., 2020; He et al., 2016; Penteado, 1983; Sinna et al., 2010; Suh et al., 2017). Despite this not being a primary concern in our study we could find a remarkable consistency in the emergence of the SCIA from either the common femoral artery or superficial femoral artery and there was no instance of the described, rare variations in origin (deep femoral artery, lateral circumflex femoral artery) (Suh et al., 2017). We found a clinically important point in the presence, in each specimen, of a clearly defined deep branch of the SCIA that runs underneath the deep fascia up to the lateral border of the sartorius muscle. This contrasts findings by other authors (Gandolfi et al., 2020; Hsu et al., 2007; Sinna et al., 2010) but is described in a more recent publication focusing especially on the deep branch (Yoshimatsu et al., 2019a, 2019b). We believe that our method, based on specimen harvesting in a deep, subfascial plane and anterograde dissection of the main pedicle after selective injection is better suited to address the perceived variations of the deep branch anatomy. While recently the importance of the deep branch for the perfusion of muscle (sartorius) and bone tissue (iliac crest) and therefore its potential for designing chimeric SCIP flaps has been analyzed (Yoshimatsu et al., 2019a, 2019b), there is little data

on the deep branch as a pedicle for perforator-based skin flaps. We therefore focused in our study on the supply of purely cutaneous flaps, relying only on perforators from each individual branch. In combination with the analysis of the different planes of elevation, our study complements the understanding of the deep branch's potential benefits and drawbacks and provides the necessary data to allow for potential chimeric flaps designed solely on the deep branch, with its longer pedicle, therefore adding potential clinical benefit.

4.2. Angiosomes and perforators

Inherently no purely anatomical study can determine to an exact extent the maximal perfusion area of a flap since vascular anastomoses are perfused to varying degrees in injection studies. Hence, only the primary angiosome (3D cutaneous tissue area encompassed by the contrasted respective branch of the SCIA) was considered in the measurement of the perfused area. Although linking vessels and choke anastomoses will lead to an increased area of vital tissue in vivo, it is reasonable to assume that the safest way to ensure flap survival is to base it on the primary angiosome of the supplying vessel.

Despite anatomical variations in perforator distribution, both branches offer areas of tissue that are always perfused and a generally constant and similar number of perforators. Planning the flap based on these regions as are illustrated in Fig. 4 should lead to a well perfused flap in vivo. Also, our analysis of the 100% perfused area based on superposition of the flaps' angiosomes and affine transformations show that flaps of 34.0 $\pm$ 8.8 cm^2 on the superficial branch respectively 34.8 $\pm$ 6.0 cm^2 on the deep branch can be always reliably harvested. The mean total angiosome is however significantly larger and in our findings the deep branch angiosome is larger on average than the superficial branch angiosome. This finding contrasts with the results of a more recent study that used selective colored injection to determine angiosome area (Gandolfi et al., 2020). We believe that our method of purely intravascular injection and CT-based imaging analysis is more reliable as it does not depend on choke vessels and allows for visualizing flap extent that is not visible through the skin.

Although the SCIA-perforators are scattered over the whole groin region, main branch perforators actually accumulate in distinct clusters, very much comparable to the situation in other flaps (Choi et al., 2007; Schaverien and Saint-Cyr, 2008; Yu et al., 2011). In most cases, it would be desirable to plan the flap based on these main perforators in order to ensure sufficient perfusion of the flap. This distribution might also explain clinical observations of flap necrosis in the very medial or distal parts of SCIP-flaps based on superficial branch perforators (Hong et al., 2013; Suh et al., 2017). There is a clear difference in the location of the perforators from the superficial and deep SCIA branch as well as in the further expansion of the respective angiosomes and flap design should be adapted according to the preferred pedicle.

A number of authors prefer perforators from the superficial branch to the ones of the deep branch, in order to avoid potential intramuscular dissection of the pedicle (Goh et al., 2015; Green et al., 2013; Suh et al., 2017). As previously stated, an important and constant finding in our study was that while the deep branch did run subfascially over the sartorius muscle and gave off nurturing vessels to this muscle, the main perforator supplying the superficial plane and skin never penetrated the muscle itself in our specimens. This suggests that in most cases the SCIP flap could be harvested without any tedious intramuscular dissection when based on the main perforator of the deep branch. These findings are consistent with some recently described surgical techniques for safe harvesting of deep branch based chimeric flaps (Yoshimatsu et al., 2019b) but contrast findings of other authors (Gandolfi et al., 2020; Sinna et al., 2010) who analyzed the perforators of the deep and superficial branches of the SCIA describing all deep branch perforators as musculocutaneous (penetrating the sartorius muscle). We believe our method of perforator dissection after strict intravascular injection with the colored and hardened dye is better suited for the assessment of the course of the deep branch's cutaneous perforators.

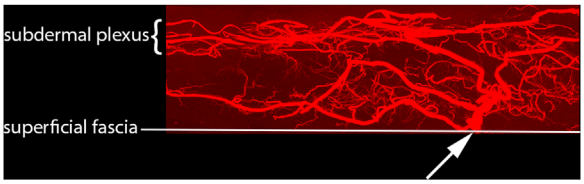

Fig. 7. Micro-CT-scan of a superficial branch perforator in the upper part of the thigh: the flap was harvested on the superficial fascia in order to ensure the correct identification of this plane. The white arrow indicates the location where the artery penetrates the superficial fascia, before branching into multiple smaller vessels. While some of those branches directly anchor to the subdermal plexus others stay more deeply, running along the superficial fascia.

4.3. Planes of elevation and layer thickness

As illustrated by our maps, the subfascial, suprafascial and superficial planes show distinct patterns with interindividual consistency. Depending on the location and plane of elevation, significantly different results in layer thickness can be achieved. The superficial plane does not only offer a thinner but also significantly more homogeneous flap, a finding underlying the importance of perforator based SCIP flap raising in order to achieve a consistent and thin flap.

The plane of elevation furthermore could impact the blood supply of the flap. It has been clinically shown that the suprafascial flap harvest does not adversely influence flap survival compared to the subfascial plane (Abdelrahman et al., 2018). While here no major difference in the vascular tree is to be expected, the superficial plane leads to the loss of direct linking vessels on the deep fascia as described by Saint-Cyr et al. (2009a, 2009b), which in turn might lead to reduced flap survival. Our micro-CT scans however did reveal suprafascial vessels in the superficial plane in regions where the superficial fascia and superficial fat content were prominent (Fig. 7). Previous descriptions of the blood supply of this plane have assumed that it is exclusively based on indirect linking vessels in the subdermal plexus (Goh et al., 2015; Hong et al., 2014). Yet these findings suggest that suprafascial direct linking vessels are at least partially involved in the blood supply of this plane too. This should be considered, especially when further debulking of superficially harvested flaps is performed.

A main finding of our study is the relationship between planes of elevation, layer thickness and flap size for the superficial versus deep branch of the SCIA.

The deep branch offers a significantly longer pedicle (mean 9.1 $\pm$ 1.0 cm) and also a larger angiosome on average. A flap based on it should be planned inferior and lateral to the inguinal ligament and can extend onto the lateral proximal thigh. If a large flap is needed the superficial harvesting plane should be employed since it not only leads to a significantly thinner but also more homogenous flap. If however, only a small flap is needed it can be positioned inferio-lateral to the inguinal ligament and can be raised above the deep fascia since it won't impact the flap's thinness significantly and insures the harvesting of all perforators and not just the main branch perforator.

The superficial branch has generally been better studied in the current literature and is the preferred SCIP pedicle for most authors (Hong et al., 2013; Hsu et al., 2007; Koshima et al., 2004). We have

found that this pedicle is in general shorter but of sufficient length for most reconstructions (6.6 ± 1.1 cm) and the flap angiosome is also significantly reduced in comparison to the deep branch. Of utmost importance is the plane of elevation in this case. Since the principal flap perforators are located in the more medial and superior aspects of the groin region this flap should be raised in a superficial plane in order to greatly reduce its bulk and increase flap homogeneity regardless whether a large or small flap is needed.

Our study provides a detailed description and comparison of the vascular pedicle of both the superficial and the deep system of the SCIP flap. We feel that our data corroborates with most recent clinical works showing the importance of flap raising in the plane of the superficial fascia. However, contrasting some preferred techniques published in the literature our study shows that the deep branch of the SCIA offers a larger flap with a longer pedicle, aspects that can prove beneficial in many clinical reconstructive surgical situations.

5. Conclusion

Our anatomical study shows that the SCIP flap has a reliable vascularity. The main pedicle and its deep and superficial branches show remarkable anatomical consistency and the spatial distribution of their perforators is clustered in definable but disparate locations. The superficial flap raising plane leads to a thin and homogenous flap with good, perforator-based vascularization. The deep branch of the SCIA provides a larger flap with a longer pedicle compared to the superficial branch and therefore could be used more frequently as a SCIP pedicle. Ultimately, only clinical experience will show if these anatomical findings are translatable to reconstructive surgical practice.

Funding sources

This research did not receive any specific grant from funding agencies in the public, commercial, or not-for-profit sectors.

Acknowledgements

We thank all donors for their willingness to support our research. Furthermore, we thank Nane Boemke for her help with the cadavers and Fluri Wieland for his assistance and expertise in the statistical evaluations.

References

Abdelrahman, M., Zelken, J., Huang, R.-W., Hsu, C.-C., Lin, Chih-Hung, Lin, Y.-T., Lin, Cheng-Hung, 2018. Suprafascial dissection of the pedicled groin flap: a safe and practical approach to flap harvest. Microsurgery 38, 458–465, http://dx.doi.org/10.1002/micr.30238.

Bangerter, H., Boemke, S., Röthlisberger, R., Schwartz, V., Bergmann, M., Müller, M.D., Djonov, V., 2017. Combined maceration procedure permits advanced microsurgical dissection of Thiel-embalmed specimens. Ann. Anat. 210, 9–17, http://dx.doi.org/10.1016/j.aanat.2016.10.008.

Bergeron, L., Tang, M., Morris, S.F., 2006. A review of vascular injection techniques for the study of perforator flaps. Plast. Reconstr. Surg. 117, 2050–2057, http://dx.doi.org/10.1097/01.prs.0000218321.36450.9b.

Choi, S.-W., Park, J.-Y., Hur, M.-S., Park, H.-D., Kang, H.-J., Hu, K.-S., Kim, H.-J., 2007. An anatomic assessment on perforators of the lateral circumflex femoral artery for anterolateral thigh flap. J. Craniofac. Surg. 18, 866–871, http://dx.doi.org/10.1097/scs.0b013e3180a03304.

Daniel, R.K., Taylor, G.I., 1973. Distant transfer of an island flap by microvascular anastomoses: a clinical technique. Plast. Reconstr. Surg. 52, 111–117, http://dx.doi.org/10.1097/00006534-197308000-00001.

Feng, S., Xi, W., Zhang, Z., Tremp, M., Schaefer, D.J., Sadigh, P.L., Zhang, W., Zhang, Y.X., 2017. A reappraisal of the surgical planning of the superficial circumflex iliac artery perforator flap. J. Plast. Reconstr. Aesthetic Surg. 70, 469–477, http://dx.doi.org/10.1016/j.bjps.2016.11.025.

Gandolfi, S., Postel, F., Auquit-Auckbur, I., Boissière, F., Pelissier, P., Casoli, V., Duparc, F., 2020. Vascularization of the superficial circumflex iliac perforator flap (SCIP flap): an anatomical study. Surg. Radiol. Anat. 42, 473–481.

Goh, T.L., Park, S.W., Cho, J.Y., Choi, J.W., Hong, J.P., 2015. The search for the ideal thin skin flap: superficial circumflex iliac artery perforator flap–a review of 210 cases. Plast. Reconstr. Surg. 135, 592–601.

Green, R., Rahman, K.M.A., Owen, S., Paleri, V., Adams, J., Ahmed, O.A., Ragbir, M., 2013. The superficial circumflex iliac artery perforator flap in intra-oral reconstruction. J. Plast. Reconstr. Aesthetic Surg. 66, 1683–1687, http://dx.doi.org/10.1016/j.bjps.2013.07.011.

Han, H.H., Lee, J.H., Kim, S.M., Jun, Y.J., Kim, Y.J., 2016. Scrotal reconstruction using a superficial circumflex iliac artery perforator flap following Fournier's gangrene. Int. Wound J. 13, 996–999, http://dx.doi.org/10.1111/iwj.12353.

He, Y., Jin, S., Tian, Z., Fang, Z., Ma, C., Tao, X., Zhang, Y., Qiu, W., Zhang, Z., Zhang, C., 2016. Superficial circumflex iliac artery perforator flap's imaging, anatomy and clinical applications in oral maxillofacial reconstruction. J. Craniomaxillofac. Surg. 44, 242–248, http://dx.doi.org/10.1016/j.jcms.2015.12.002.

Hlushchuk, R., Zubler, C., Barré, S., Correa Shokiche, C., Schaad, L., Röthlisberger, R., Wnuk, M., Daniel, C., Khoma, O., Tschanz, S.A., Reyes, M., Djonov, V., 2018. Cutting-edge microangio-CT: new dimensions in vascular imaging and kidney morphometry. Am. J. Physiol. Ren. Physiol. 314, F493–F499, http://dx.doi.org/10.1152/ajprenal.00099.2017.

Hong, J.P., Sun, S.H., Ben-Nakhi, M., 2013. Modified superficial circumflex iliac artery perforator flap and supermicrosurgery technique for lower extremity reconstruction: a new approach for moderate-sized defects. Ann. Plast. Surg. 71, 380–383, http://dx.doi.org/10.1097/SAP.0b013e3182503ac5.

Hong, J.P., Choi, D.H., Suh, H., Mukarramah, D.A., Tashti, T., Lee, K., Yoon, C., 2014. A new plane of elevation: the superficial fascial plane for perforator flap elevation. J. Reconstr. Microsurg. 30, 491–495, http://dx.doi.org/10.1055/s-0034-1369807.

Hough, M., Fenn, C., Kay, S.P., 2004. The use of free groin flaps in children. Plast. Reconstr. Surg. 113, 1161–1166, http://dx.doi.org/10.1097/01.PRS.0000110329.68009.4C.

Hsu, W.M., Chao, W.N., Yang, C., Fang, C.L., Huang, K.F., Lin, Y.S., Lee, T.H., 2007. Evolution of the free groin flap: the superficial circumflex iliac artery perforator flap. Plast. Reconstr. Surg. 119, 1491–1498, http://dx.doi.org/10.1097/01.prs.0000256057.42415.73.

Iida, T., 2014. Superficial circumflex iliac perforator (SCIP) flap: variations of the SCIP flap and their clinical applications. J. Reconstr. Microsurg. 30, 505–508, http://dx.doi.org/10.1055/s-0034-1370360.

Iida, T., Mihara, M., Yoshimatsu, H., Narushima, M., Koshima, I., 2013. Reconstruction of the external auditory canal using a super-thin superficial circumflex iliac perforator flap after tumour resection. J. Plast. Reconstr. Aesthet. Surg. 66, 430–433, http://dx.doi.org/10.1016/j.bjps.2012.08.005.

Iida, T., Mihara, M., Yoshimatsu, H., Narushima, M., Koshima, I., 2014. Versatility of the superficial circumflex iliac artery perforator flap in head and neck reconstruction. Ann. Plast. Surg. 72, 332–336, http://dx.doi.org/10.1097/SAP.0b013e318260a3ad.

Kim, J.H., Kim, K.N., Yoon, C.S., 2015. Reconstruction of moderate-sized distal limb defects using a superthin superficial circumflex iliac artery perforator flap. J. Reconstr. Microsurg. 31, 631–635, http://dx.doi.org/10.1055/s-0035-1558959.

Koshima, I., Nanba, Y., Tsutsui, T., Takahashi, Y., Urushibara, K., Inagawa, K., Hamasaki, T., Moriguchi, T., 2004. Superficial circumflex iliac artery perforator flap for reconstruction of limb defects. Plast. Reconstr. Surg. 113, 233–240, http://dx.doi.org/10.1097/01.PRS.0000095948.03605.20.

Koshima, I., Nanba, Y., Nagai, A., Nakatsuka, M., Sato, T., Kuroda, S., 2006. Penile reconstruction with bilateral superficial circumflex iliac artery perforator (SCIP) flaps. J. Reconstr. Microsurg. 22, 137–142, http://dx.doi.org/10.1055/s-2006-939957.

McGregor, I.A., Jackson, I.T., 1972. The groin flap. Br. J. Plast. Surg. 25, 3–16, http://dx.doi.org/10.1016/S0007-1226(72)80003-1.

Myung, Y., Yim, S., Kim, B.-K., 2017. A comparison of axial circumference between superficial circumflex iliac artery perforator flap and other workhorse flaps in dorsal foot reconstruction. J. Plast. Surg. Hand Surg. 51, 381–386, http://dx.doi.org/10.1080/2000656X.2017.1279621.

Penteado, Cv., 1983. Anatomosurgical study of the superficial and deep circumflex iliac arteries. Anat. Clin. 5, 125–127, http://dx.doi.org/10.1007/BF01798983.

Rueden, C.T., Schindelin, J., Hiner, M.C., DeZonia, B.E., Walter, A.E., Arena, E.T., Eliceiri, K.W., 2017. ImageJ2: ImageJ for the next generation of scientific image data. BMC Bioinformatics 18, 529, http://dx.doi.org/10.1186/s12859-017-1934-z.

Saint-Cyr, M., Schaverien, M., Wong, C., Nagarkar, P., Arbique, G., Brown, S., Rohrich, R.J., 2009a. The extended anterolateral thigh flap: anatomical basis and clinical experience. Plast. Reconstr. Surg. 123, 1245–1255, http://dx.doi.org/10.1097/PRS.0b013e31819e2718.

Saint-Cyr, M., Wong, C., Schaverien, M., Mojallal, A., Rohrich, R.J., 2009b. The perforasome theory: vascular anatomy and clinical implications. Plast. Reconstr. Surg. 124, 1529–1544, http://dx.doi.org/10.1097/PRS.0b013e3181b98a6c.

Schaad, L., Hlushchuk, R., Barré, S., Gianni-Barrera, R., Haberthür, D., Banfi, A., Djonov, V., 2017. Correlative imaging of the murine hind limb vasculature and muscle tissue by MicroCT and light microscopy. Sci. Rep. 7, http://dx.doi.org/10.1038/srep41842.

Schaverien, M., Saint-Cyr, M., 2008. Perforators of the lower leg: analysis of perforator locations and clinical application for pedicled perforator flaps. Plast. Reconstr. Surg. 122, 161–170, http://dx.doi.org/10.1097/PRS.0b013e3181774386.

Sinna, R., Hajji, H., Qassemyar, Q., Perignon, D., Benhaim, T., Havet, E., 2010. Anatomical background of the perforator flap based on the deep branch of the superficial circumflex iliac artery (SCIP Flap): a cadaveric study. Eplasty 10, e11.

Suh, H.S.P., Jeong, H.H., Choi, D.H., Hong, J.P.J.P., 2017. Study of the medial superficial perforator of the superficial circumflex iliac artery perforator flap using computed tomographic angiography and surgical anatomy in 142 patients. In: Plastic

and Reconstructive Surgery. Lippincott Williams and Wilkins, pp. 738–748, http://dx.doi.org/10.1097/PRS.0000000000003147.

Thiel, W., 1992. The preservation of the whole corpse with natural color. Ann. Anat. 174, 185–195.

Yoshimatsu, H., Steinbacher, J., Meng, S., Hamscha, U.M., Weninger, W.J., Tinhofer, I.E., Harima, M., Fuse, Y., Yamamoto, T., Tzou, C.H.J., 2019a. Superficial circumflex iliac artery perforator flap: an anatomical study of the correlation of the superficial and the deep branches of the artery and evaluation of perfusion from the deep branch to the sartorius muscle and the iliac bone. Plast. Reconstr. Surg. 143, 589–602, http://dx.doi.org/10.1097/PRS.0000000000005282.

Yoshimatsu, H., Yamamoto, T., Hayashi, A., Fuse, Y., Karakawa, R., Iida, T., Narushima, M., Tanakura, K., Weninger, W.J., Tzou, C.H.J., 2019b. Use of the transverse branch of the superficial circumflex iliac artery as a landmark facilitating identification and dissection of the deep branch of the superficial circumflex iliac artery for free flap pedicle: anatomical study and clinical applications. Microsurgery 39, 721–729, http://dx.doi.org/10.1002/micr.30518.

Yu, P., Chang, E.I., Hanasono, M.M., 2011. Design of a reliable skin paddle for the fibula osteocutaneous flap: perforator anatomy revisited. Plast. Reconstr. Surg. 128, 440–446, http://dx.doi.org/10.1097/PRS.0b013e31821e7058.